

Charging Stations Distribution Optimization using Drones Fleet for Disaster Prone Areas Original Article

Zohaib Hassan¹, Irtiza Ali Shah², Ahsan Sarwar Rana³

^{1,3}Electrical and Computer Engineering Department, Air University, Islamabad, Pakistan

²Department of Mechanical and Aerospace Engineering, Air University, Islamabad, Pakistan

* **Correspondence:** Zohaib Hassan, zohaib.hassan@mail.au.edu.pk

Citation | Hassan. Z, Shah. A. I, Sarwar. R. A, "Charging Stations Distribution Optimization using Drones Fleet for Disaster Prone Areas," Int. J. Innov. Sci. Technol., vol. 4, no. 5, pp. 103-121, 2022.

Received | June 4, 2022; **Revised** | June 20, 2022; **Accepted** | June 28, 2022; **Published** | June 30, 2022.

A disaster is an unforeseen calamity that causes damage to property or brings about a loss of human life. Quick response and rapid distribution of vital relief items into the affected region could save precious lives. In this regard, disaster management comes into play, which is highly dependent on the topography of the disaster-hit area. If the disaster-hit area has little or no road connectivity, the use of drones in such areas becomes essential for the delivery of health packages. Since the battery capacity of the drone is limited, there is a need of charging stations that should be transported using road infrastructure and pre-installed in disaster-prone areas, as access to these areas may be denied once the disaster hits. In this article, a simulation model was used to optimize the number and location of drone charging stations for deployment in a disaster-prone area in the pre-disaster scenario, aiming at the distribution of relief items to disaster-hit areas in the post-disaster scenario. We consider the relative priority of locations where a preference is given to the locations that have higher priority levels. An optimal number of charging stations and optimal routes have also been determined by using our optimization model. To illustrate the use of our model, numerical examples have been simulated for different sizes of the disaster-hit area and the number of targets. In our numerical simulation, it was observed that the drone's maximum distance capacity is the key factor in determining the optimal grid size, which directly correlates to the number of charging stations.

Keywords: Drone Charging Stations, Disaster Preparedness, and Response, Drone Path Planning, Energy Optimization, Drone Recharging

Author's Contribution.

All authors came up with the initial concept. Modelling and first draft preparation was done by Zohaib Hassan. Editing and proofreading was done by Irtiza Ali Shah and Ahsan Sarwar Rana. All authors read and approved the final manuscript.

Conflict Of Interest:

The authors declare that the manuscript has not been published or submitted to other journals previously and there are no conflicts of interest.

Project details.

The Authors declare that this research was not conducted as a result of any project.

Introduction

Recent disasters have caused significant economic and human losses, such as earthquakes in Iran (2003, 2017) and Chile (2011, 2015), and tsunamis in Japan (2011) [1]. There is a high rate of fatality that results from a shortage of relief items following a disaster [2]. In such situations, quick response and rapid distribution of vital relief items into affected regions could prevent suffering and life loss. Relief items consist of the essential requirements of the affected people, such as food, water, tent, clothing, etc. The main challenges of relief items distribution are associated with means of transport and transport infrastructure. Humanitarian aid agencies are often confronted with poor, inexistent, or destroyed road infrastructure in disaster-hit areas. Road networks may be disrupted due to flooding, blockade, bridge collapses, and debris [3]. In these situations, unmanned aerial vehicles drones can provide solutions to the problems associated with the distribution of relief items.

Drones have many applications, but they also come up with some limitations. The limited battery capacity of the drones puts a limit on the maximum distance that a drone can travel. There is a need for charging stations, which can be used by the drones to recharge the battery, as the battery capacity of the drone is limited. The charging stations should be transported using road infrastructure and pre-installed in the disaster-prone area, as access may be denied once it is hit with disaster. In the post-disaster phase, the already-installed charging stations can then be used by drones to recharge their batteries.

In the literature, we find several studies that address the problem of distributing relief items in a disaster setting. Macias [4] presented an endogenous stochastic vehicle routing problem model, in which a drone provides information to the ground vehicle for the distribution of relief items. The location of depot facilities is also crucial for the efficient flow of relief items. In this regard, different models have been proposed. Maghfiroh [5] proposed a multimodal relief distribution model that determined the optimal locations of depots. Chowdhury [6] presented a continuous approximation model to determine the optimal depot locations. Wei [7] proposed an integrated-location routing problem for depot selection and vehicle assignment. Wei [7] proposed an integrated-location routing problem for depot selection and vehicle assignment. The models proposed by Moshref-javadi and Lee [8], Wei [7], and Davoodi and Goli [9] examine the simultaneous Location routing problems for supply distribution operations. Some studies in the literature focus on multiple sources of transportation for relief distribution. Ertem [10] concluded that the use of multimodal and intermodal transportation could be alternatives if relief distribution cannot be accomplished using a single infeasible mode.

It is essential to determine the type, number, and location of the demand areas for timely delivery of relief supplies. In this regard, Sebatli [11] presented a simulation-based approach to determine the demand of disaster-hit areas and appropriately assign depot locations. Faiz [12] presented a two-echelon vehicle routing computational framework. In this work, a hotspot drone captured the demand by providing communication capabilities to the disaster-hit area, and a delivery drone satisfied the demand. Rivera-Royero [13] proposed a rolling horizon methodology that considered dynamic parameters, such as demand quantity, capacities of drones, and demand priorities, for the distribution of relief items by including relief goods. This methodology also included assembling activities before the delivery of items. Lu [14] developed a real-time relief distribution model for disaster response that includes a demand and time estimator as well as a module for solving optimal distribution flows.

In literature, we find studies that consider factors such as the state of the road, which affects the delivery time. Hu [15] proposed a multi-stage stochastic programming model for disaster relief distribution that considered multiple vehicle types and the state of the road network. Sabouhi [16] considered the expected arrival time of relief vehicles to the disaster-hit

areas keeping into consideration the disruptions caused due to disasters. Baskaya [17] used different route distances between centers and affected locations to reveal the disruption levels of the road network. Moreno [18], and Ferrer [19] used binary variables to describe the state of arcs (road paths) in the relief distribution problems. Penna [20] recently used the concept of rich vehicle routing and considered accessibility constraints that allowed only compatible vehicles to serve particular routes owing to road blockage or geographical conditions. Some studies in the literature discuss the effects of a drone's flight-related parameters. Kim [21] presented a stochastic modeling framework to determine the locations of drone facilities and transport capacities of drones for effectively handling the disaster. Baharmand [22] proposed a location-allocation model that considered the capacity of facilities and vehicle fleets and enabled decision-makers to determine trade-offs between response time and logistics costs. Rottondi [23] explored the joint planning of multitasking missions using a fleet of UAVs that were equipped with a standard set of accessories/tools, which enabled heterogeneous tasks.

For long-distance flying, drones often need to charge their battery at battery-charging stations because of their limited battery capacity. In the literature, we find studies that have focused on the deployment of charging stations to address the issue of the limited flight time of drones. Myounggyu Won [24] addressed the problem of deploying charging stations that maximizes the system performance, specifically concentrating on generating optimal UAV trajectories while minimizing the number of deployed charging stations. Hailong Huang [25], considered the approach of deploying charging stations and collaborating with public transportation vehicles. Yujie Qin [26] [27] used tools from queuing theory and stochastic geometry to study the influence of each of the charging station's limited capacity and spatial density on the performance of a drone-enabled wireless network. Yujie Qin [28] investigated the possibility and performance enhancement of the deployment of renewable energy (RE) charging stations. The authors used simulation results to demonstrate that RE charging stations can be a possible solution to address the limited onboard battery of UAVs in rural areas. Xiaoshan Lin [29] considered persistent (long-horizon) surveillance over an environment by using energy-constrained unmanned aerial vehicles (UAVs), which are supported by unmanned ground vehicles (UGVs) serving as mobile charging stations. The goal is to periodically visit a set of monitoring points by the UAVs while minimizing the maximum time between consecutive visits to any of those points. Yujie Qin [30] studied the performance of a UAV-enabled cellular network while capturing the influence of the spatial distribution of the charging stations. In particular, the author used tools from stochastic geometry to derive the coverage probability of a UAV-enabled cellular network as a function of the battery size, the density of the charging stations, and the time required for recharging/replacing the battery.

The work proposed in [31] is the most relevant to our work. We have used this work to validate our approach. Huang H and Savkin A [31] proposed a model to investigate the deployment of several charging stations to cover the customers in an urban demand area. In this model, the location coordinates of the target areas are already known. The charging stations covering no or fewer target locations are removed. Therefore, some areas are not reachable by drone. Our study aims to develop a mathematical model and use existing techniques to optimize drone delivery of relief items to disaster-hit areas considering the technical specifications of UAVs/drones. The proposed model considers drone energy consumption as a function of the payload and Euclidean distance. In our proposed model, the target locations are unknown, so we performed our simulation using random target locations. In this paper, we present a novel optimization model to optimize the location and number of charging stations for the pre-disaster phase. The relative priority of locations is attributed and a preference is given to the disaster-hit area with higher priority levels. The routes of drones

are optimized for the post-disaster phase. Figure 1 shows the step-by-step flow of study diagram for our research.

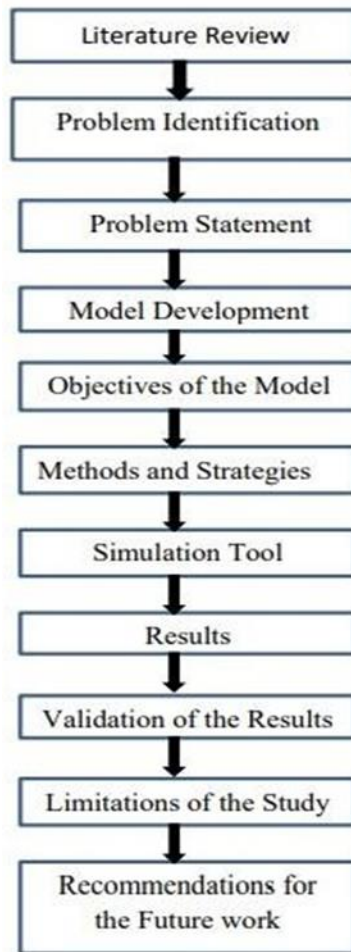


Figure 1. Flow of study diagram for our research

The remainder of this paper is organized as follows. In Section II, the cost function and constraints are defined to build the optimization model. Section III presents the methods used for clustering, drone allocation to the clusters, grouping, and path planning. In Section IV, the simulation results of numerical examples are discussed. A short discussion on future research concludes the paper.

Problem Formulation

In this section, we have discussed all the parameters of our model. Let us say we have a set of target/disaster-hit locations $\check{T} = \{T_1, T_2, \dots, T_M\}$ and a set of drone charging stations $\check{R} = \{R_1, R_2, R_3, \dots, R_C\}$, where M and C are the numbers of target/disaster-hit locations and drone charging stations, respectively. Let the set of base stations $\check{H} = \{H\}$ be a singleton set. $Y = \check{T} \cup \check{R} \cup \check{H}$ is the set of all locations in the system. We assume that the target locations are of low-, medium-, and high-priority categories. K is the number of clusters into which the target locations are divided. N is the total number of drones. We have selected the Amazon Prime Air drone for our study [32]. Let S be the maximum distance that this drone can cover with a maximum payload weight and maximum battery capacity. We assume that the payload capacity of the drone is five packages, each with a weight equal to 0.46 kg. The maximum payload weight that the selected drone can carry is 2.3 kg.

We assume that the demand of every target location is $\epsilon=1$. Therefore, a drone can deliver relief packages to five target locations in one route.

Let's discuss a scenario in which a drone follows two different routes for the same target locations given in Fig. 2(a) and (b).

Let G , the grid size, be the distance between adjacent drone charging stations. The number of charging stations in a defined area depends on the value of the grid size G . For a larger value of G , we have fewer charging stations in the defined area and vice versa.

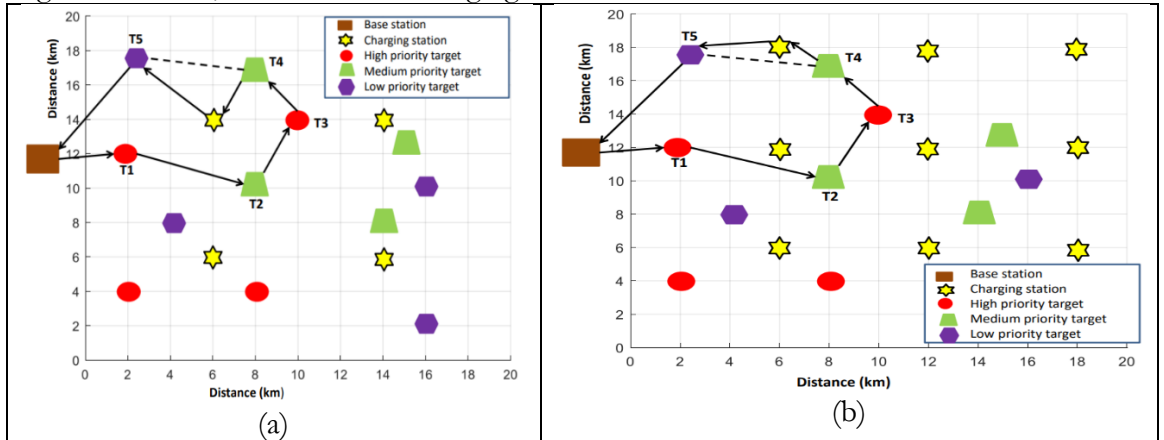


Figure 2. Proposed layout of two different drone routes for the same targets of (a) four charging stations and (b) nine charging stations

In Figure 2(a), there are four charging stations. The dotted line shows the shortest path (displacement) from target T_4 to target T_5 . Suppose the drone does not have enough energy to reach T_5 directly from T_4 . It will need to visit a nearby charging station to recharge its battery; therefore, it covers an off-track distance, as shown by the solid line in Figure 2(a). In Figure 2(b), a grid of nine charging stations is shown. In this scenario, the drone travels over a shorter off-track distance to reach the charging station from target location T_4 . When the charging stations are fewer in number, there is a higher probability that the drone travels a longer off-track distance and vice versa.

Cost Function

As discussed before, there is an inverse relationship between the number of charging stations and the distance traveled by the drone. The objective of our model is to minimize both the number of charging stations and the total traveled distance.

The cost function is defined as follows:

$$\min(10C+D) \tag{1}$$

where C is the number of charging stations, and D is the total distance. We have assumed that the cost of traveling a distance of 10 km is equal to the cost of installing one drone charging station.

Constraints

Degree Constraints

Let H be the singleton set of the base stations. \check{T} is a set of target locations, \check{R} is the set of charging stations, x_{ij} is the number of times a drone travels from location i to j , and Y is the set of all locations in the system. Degree constraints are given as follows:

We assume that each demand location in \check{T} is visited exactly once by only one drone, as given in (2).

$$\sum_{i \in Y \setminus \{j\}} x_{ij} = 1, j \in \check{T} \tag{2}$$

A drone can visit charging stations and depots as many times as required, i.e., when the drone battery is empty or for the loading of relief items. However, the number of times it enters and leaves a charging station or a depot must be equal, as given in (3).

$$\sum_{i \in Y/\{j\}} x_{ij} = \sum_{i \in Y/\{j\}} x_{ji}, j \in Y \quad (3)$$

At least one drone is used to supply relief items to demand locations in \check{T} . Therefore, the number of drones that moves x_{ij} between the depot and demand locations \check{T} or charging stations \check{R} must be greater than 0, as expressed in (4).

$$\sum_{j \in Y/H} x_{ij} > 0, i \in H \quad (4)$$

Demand Constraints

Let w_{ij} be the payload carried by the drone when it travels from location i to j . W is the total payload capacity of the drone, and c is the unit package demand. The demand constraints are given as follows:

For energy-saving purposes, the drone does not need to carry the maximum payload on each route. We impose that the drone returns to the depot empty, as expressed in (5).

$$\sum_j w_{ji} = 0, i \in H. \quad (5)$$

If the drone travels from i to j , the difference in the payload (between arrival and departure) is equal to the demand at location i , which is a unit package given in (6), except for the charging station locations given in (7).

$$\sum_j w_{ji} - \sum_j w_{ij} = c, i \in \check{T} \quad (6)$$

$$\sum_j w_{ji} - \sum_j w_{ij} = 0, i \in \check{R} \quad (7)$$

The payload on any route cannot exceed the maximum payload of the drone, as given in (8).

$$w_{ij} \leq W, i \in Y, j \in Y \quad (8)$$

Energy Constraints

Let e_{ij} be the energy level of the drone when it leaves location i to travel to j . E is the maximum battery capacity of the drone, d_{ij} is the distance between locations i and j , ρ_0 is the energy required for an empty drone to fly one unit distance, and ρ is the additional energy needed for a drone to fly one unit distance with one package. The energy constraints are given as follows:

We assume that the drone's battery is always fully charged when it leaves the depot or a charging station, as expressed in (9).

$$e_{ij} = E, i \in H \cup \check{R}, j \in Y/\{i\} \quad (9)$$

The energy level of the battery is always lower or equal to the maximum energy level E , as expressed in (10).

$$e_{ij} \leq E, i \in \check{T}, j \in Y/\{i\} \quad (10)$$

Equation (11) gives the energy balance, i.e., the amount of energy consumed to move from any location to location i in \check{T} .

$$\sum_{j \in Y/\{i\}} e_{ji} - \sum_{j \in Y/\{i\}} e_{ij} = \sum_{j \in Y/\{i\}} d_{ji}(\rho_0 + \rho w_{ji}), i \in \check{T} \quad (11)$$

The energy level in the battery when the drone leaves location i must be sufficient for it to reach any charging station \check{R} and demand location \check{T} , as expressed in (12) and (13), respectively.

$$e_{ij} \geq d_{ij}(\rho_0 + \rho w_{ij}), i \in Y, j \in \check{R} \quad (12)$$

$$e_{ij} \geq d_{ij}(\rho_0 + \rho w_{ij}) + d_{jk}(\rho_0 + \rho w_{jk}), i \in Y, j \in \check{T}, k \in \check{R} \quad (13)$$

Optimization of the Grid size

A route is completed when a drone loads payload packages from the base station and returns after delivering relief items to the target locations. A route will only be valid if it satisfies the constraints given in (2)–(13). The constraints that are given in (5), (8), (9), (10), (12), and (13) apply before a drone makes a single move. The constraints that are given in (6), (7), and (11) apply when a drone has made a single move, and the constraints given in (2), (3), and (4) apply throughout the entire route. A scenario is given in Figure 3, wherein a grid of four charging stations, $R_1, R_2, R_3,$ and $R_4,$ is shown.

Let the drone be initially present at charging station R_1 . We assume its destination be the target location T_1 , as shown in Figure 3. After reaching the destination, the drone travels to the nearby charging station R_3 . Let d_1 be the distance from charging station R_1 to the target location T_1 and d_2 be the distance from the target location T_1 to the charging station R_3 . Let Z be the distance from R_1 to R_3 . Z is the maximum possible distance that the drone might need to travel with the maximum payload. Let S be the maximum distance that the drone can travel with the maximum payload and maximum energy. Therefore, Z should be less than or equal to S for the drone to be able to reach the target location and then travel to any nearby charging station. The distance between adjacent charging stations is G , which is the grid size.

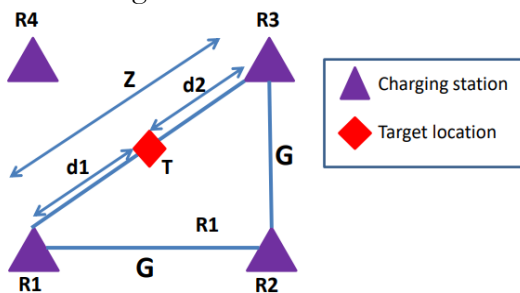


Figure 3. Proposed layout of a special scenario wherein a drone travels the maximum distance

Using Figure 2, Z can be written as

$$Z = G\sqrt{2} \quad (14)$$

Therefore, we can write the following expression:

$$G \leq \frac{S}{\sqrt{2}} \quad (15)$$

For each value of the grid size G , different values of the cost functions are determined. The optimal grid size is determined by the value of G for which the cost function is at its minimum. The optimal number of charging stations corresponds to the optimal value of the grid size for a defined area, methods, and strategies.

Assumptions in our model

We proposed a model to optimize the number of charging stations to be pre-installed in the disaster-prone area. We assume that historical data is available about the location of the disaster-prone areas, where the charging stations will be transported and installed. The charging stations will be fixed facilities. In the post-disaster phase, the location of the charging stations will not be changed concerning the location of the targets, as it will be costly and

crucial time will be lost. We assume that the mobile phones or the hot spot drone will be used to get the data on the location and the priority level of the targets. Based on the data received, locations can be given different priority level values to cater to the urgency of the relief.

Result and Discussion

We developed an algorithm for obtaining the optimal number of charging stations. The flow chart is given in Figure 4.

The drone's maximum distance capacity S is used to get the maximum valid grid size, VG_{max} , for a given size of the disaster area. The different number of charging stations are obtained for different values of the grid size in each iteration of the "for" loop, as given in Figure 3. After that, we randomly distribute low-, medium-, and high-priority targets within the defined area, as shown in Figure 5.

The next sections explain the modules of clustering, drone allocation to clusters, grouping of clusters, group ordering, and path planning/routing.

Clustering of Targets

The division of a larger number of target locations into smaller units is termed as clustering. We used the k-means algorithm, which is based on the Euclidean distances between them. Initially, we select K random points as initial centroids. Then, K clusters are formed by assigning all targets to the closest centroids. Subsequently, centroids are recalculated by finding the Euclidean mean of the clusters. This process is repeated until the centroids do not change. Fig. 6 shows the division of target locations into clusters.

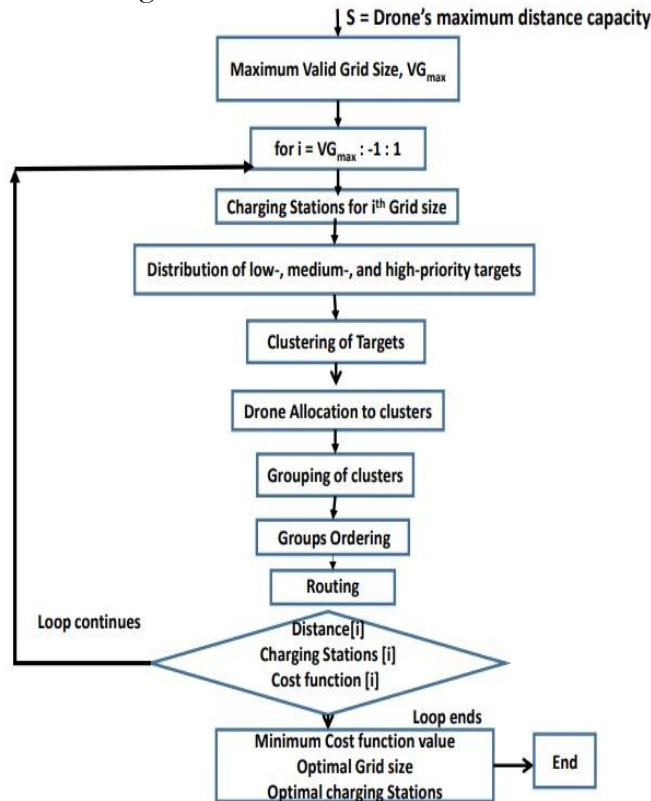


Figure 4. Flow chart of the proposed algorithm for determining optimal charging stations

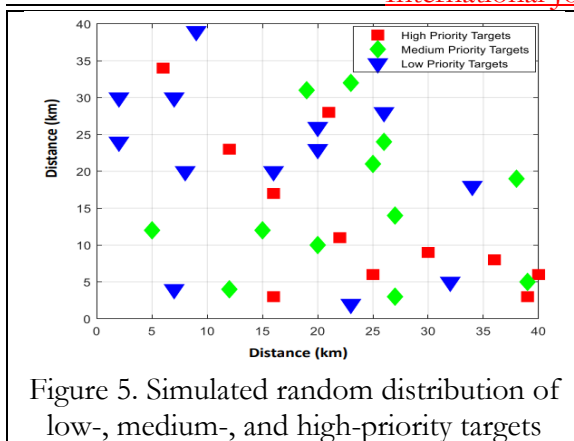


Figure 5. Simulated random distribution of low-, medium-, and high-priority targets

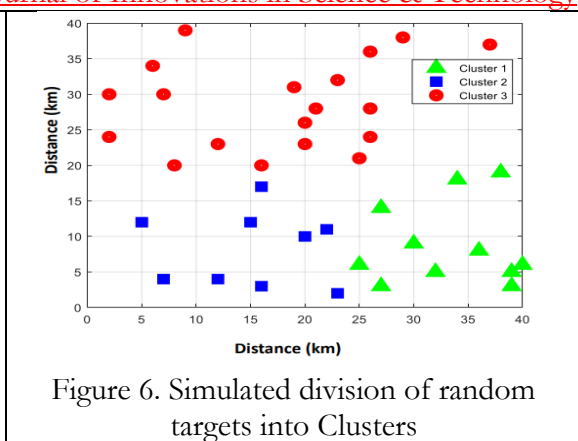


Figure 6. Simulated division of random targets into Clusters

Drone Allocation to Clusters

Drone allocation is based on the cardinality of the clusters. The expression to calculate the number of drones for each cluster is given below:

$$V_k = \frac{t_k N}{M} \quad (16)$$

Where t_k is the number of targets in the k^{th} cluster, M is the total number of targets, N is the total number of drones, and V_k is the number of drones allocated to the k^{th} cluster; the value of V_k is rounded off to the nearest integer value.

Grouping

The clusters are divided into groups of five targets each. The objective of making groups is to first visit those targets that are closer to each other and have a higher priority level value. Hence, the drone covers a shorter distance and covers more high-priority areas, also achieving a greater summed priority score if all priority values of the visited group are summed.

Selection of the first and second target of a group

The base station is taken as the reference location for selecting the first target of a group. The distance between every target in a cluster and the base station is calculated. In Figure 7, the arrows indicate the distances between each target and the base station. The shortest distance is termed d_{min} .

First, we calculate the value of α_i for the i^{th} target in a cluster using (17).

$$\alpha_i = \frac{d_{min}}{d_{HTi}} \quad (17)$$

In equation (17), d_{HTi} is the distance between the i^{th} target and the base station, and d_{min} is the distance of the target that is closest to the base station. The value of α_i for the i^{th} target is at its maximum for the closest target from the base station.

β_i is the priority of the i^{th} target, as given in (18), which is at a maximum for a high-priority target.

$$\delta_i = \alpha_i \beta_i \quad (18)$$

The target with the highest value of δ is chosen as the first target of a group. For selecting the second target of a group, the location of the first target is considered as the reference location instead of the base station.

Selection of the third, fourth and fifth target of a group

The first and second selected targets are taken as the references for the selection of the remaining three targets to complete a group. The sum of the distances of the i^{th} target from the first and second selected targets is calculated. The arrows shown in Fig. 8 indicate the distances of the i^{th} target from the first and second selected targets.

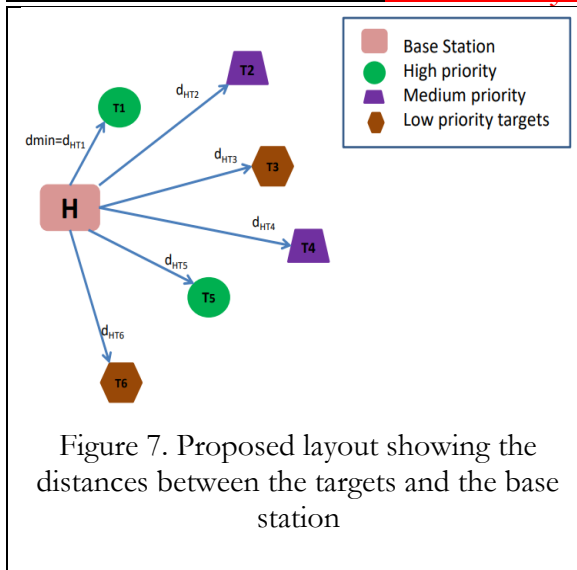


Figure 7. Proposed layout showing the distances between the targets and the base station

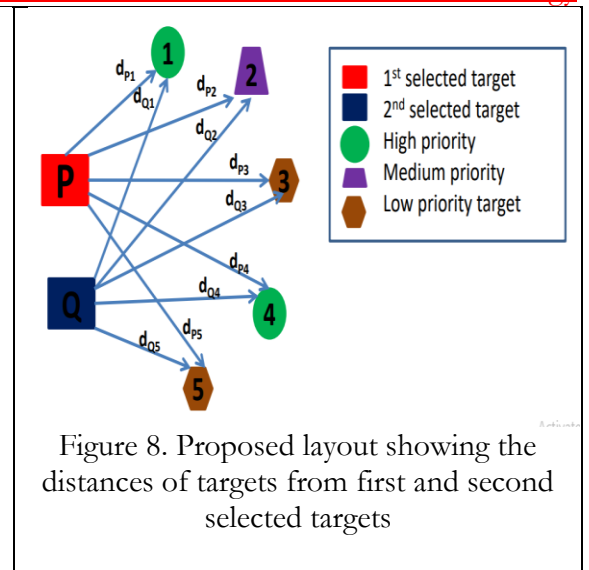


Figure 8. Proposed layout showing the distances of targets from first and second selected targets

In Figure 7, P and Q are the first and second selected targets, respectively, as shown in Figure 6, where d_{pi} is the distance between the i^{th} target and the first selected target P, and d_{qi} is the distance between the i^{th} target and the second selected target Q. First, we calculate the value μ_i of the i^{th} target using (19).

$$\mu_i = \frac{d_{min}}{d_{qi} + d_{pi}} \quad (19)$$

where d_{min} is the minimum distance of the i^{th} target from both reference locations P and Q, d_{qi} and d_{pi} are the distances between the i^{th} target and the reference locations Q and P, respectively. μ_i of the i^{th} target location will be greater for a target that is closer to both P and Q.

β_i is the priority value of the i^{th} target, and ζ_i of the i^{th} target is calculated using the formula given in (20).

$$\zeta_i = \mu_i \beta_i \quad (20)$$

The targets with the top three values of ζ_i are selected as the remaining three target locations to complete the group of five targets. Groups of the clusters are shown in Figure 9.

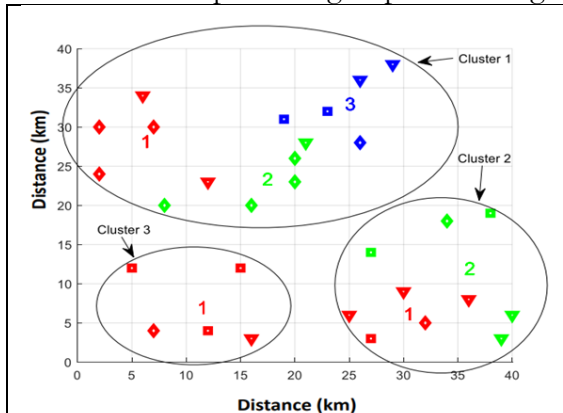


Figure 9. Simulated division of clusters into groups of five targets each. The square symbol indicates high-priority targets, the diamond symbol shows medium-priority targets, and the triangle symbol shows low-priority targets.

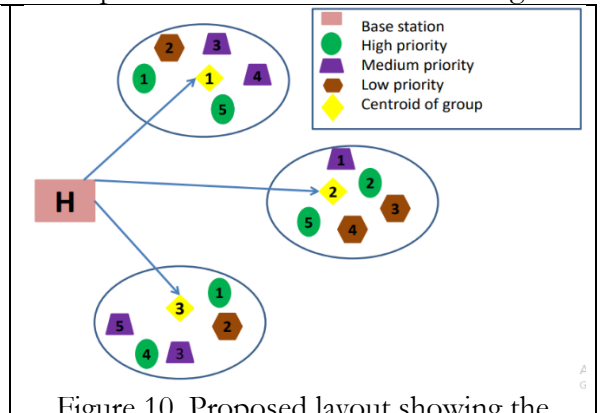


Figure 10. Proposed layout showing the distances between centroids of groups and the base station

Method to order groups

In this section, we devise a method to arrange the groups in order, so that the groups that are closer to the base station and have higher throughput are visited first. Here, summed priority score is the sum of the priority level values of the targets in a group. In Figure 10, arrows indicate distances between the centroids of groups and the base station. The value of λ_i for the i^{th} group is calculated using the expression in (21)

$$\lambda_i = \frac{d_{min}}{d_{Hi}} \quad (21)$$

where d_{min} is the closest distance between that group and the base station, d_{Hi} is the distance between the centroid of the i^{th} group and the base station, and λ is the maximum of the group for which the centroid is closest to the base station.

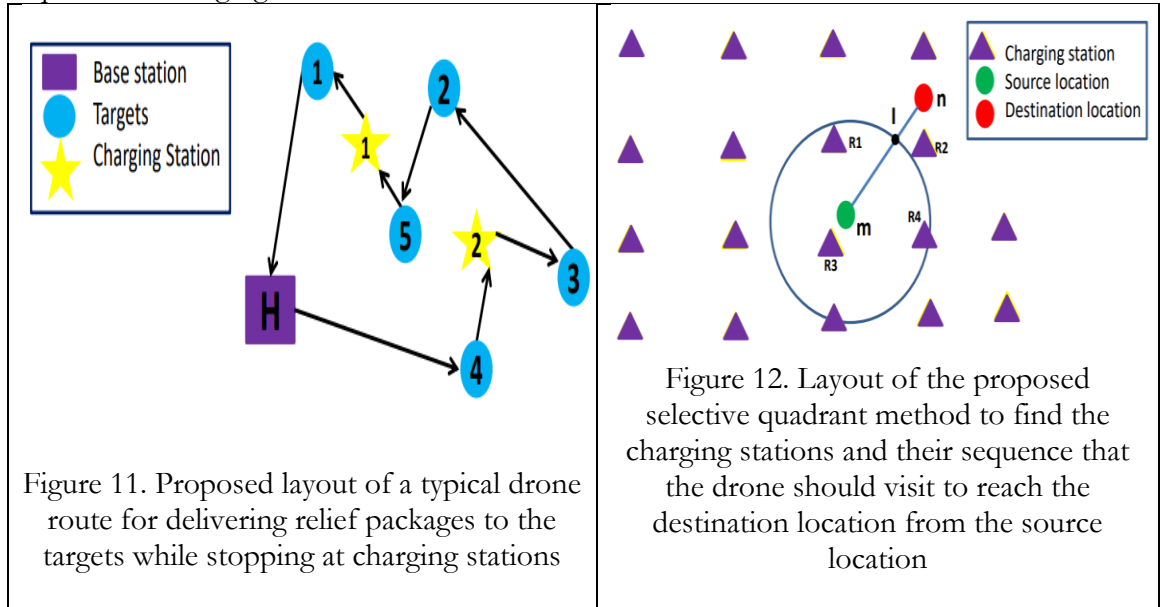
U_i is the throughput of the i^{th} group. ξ_i for the i^{th} group is calculated using (22), and the groups are arranged in descending order concerning ξ .

$$\xi_i = \lambda_i U_i \quad (22)$$

The group with the highest value of ξ is served first, and that with the lowest value of ξ is served at the end.

Path Planning/Routing

We define a route as the path followed by a drone to visit targets and return to the base station. Figure 11 shows the possible route of a drone, in which the drone visits five targets and two charging stations. Equation (13) is the energy required to visit any target location. A drone requires a charging station when it cannot reach the target destination directly. The drone may need to visit more than one charging station if the destination target is very far. We propose the use of the 'selective quadrant method' to find the number and sequence of charging stations.



In Figure 12, the source location m and the destination location n are shown. The distance that the drone can travel with its current energy is calculated, and a circle of a radius equal to that distance is drawn. Then, a line that connects m and n is drawn. This line intersects the circle at a point denoted by I , as shown in Figure 11. We select the four potential charging stations that are closest to intersection point I , denoted by $R_1, R_2, R_3,$ and R_4 in Figure 11. Only one charging station is selected, which is closest to the destination location and inside the circle boundary. If the selected charging station satisfies the energy constraint given in (13), there is

no need for more charging stations. Else, the method is repeated, and the selected charging station becomes the source location.

This method is repeated until we find a charging station that meets the constraint given in (13).

For each iteration, we get a different number of charging stations, total distance, and the value of cost function corresponding to the different values of the grid size. The optimal grid size is determined by the value of G for which the cost function is at its minimum. The optimal number of charging stations corresponds to the optimal value of the grid size for a defined area.

The algorithm given in Figure 13 determines the optimal routes using the optimal number of charging stations obtained using the algorithm given in Figure 3.

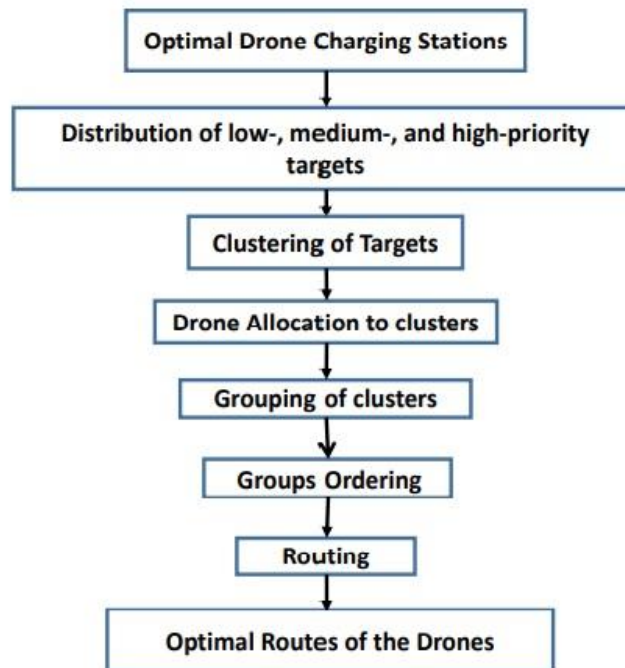


Figure 13. Flow chart of the proposed algorithm for calculation of optimal routes

Simulations and Results

In this section of the paper, we present numerical examples to illustrate the use of our proposed model. We have selected Matlab (MathWorks) tool for our simulation. We used the specifications of the Amazon Prime Air drone in our simulation, which is a hybrid drone [16]. The maximum distance that this drone can travel with a maximum payload and maximum energy is $S=16$ km. The maximum energy of the selected drone is $E=1332$ kJ.

In our simulation, there is one base station, and the targets are divided into clusters. We have assumed that the payload capacity of the drone is $W=5$ packages. The demand at each target is $c=1$ package. Each target is assigned a value based on its priority level. The high-priority value is equal to 1, the medium-priority value is 0.7, and the low-priority value is 0.4. Initially, the drones are located at the base station at the start of the delivery process. The process of simulation is explained as follows.

The targets are divided into clusters (Explained in Section 3.1). The clusters are divided into groups of 5 targets each (Explained in Section 3.3). Initially, the maximum valid value of the grid size is calculated using the expression given in (15). The grid size value determines the number of charging stations. The route of the drone is completed when it

departs from the base station and returns after visiting five targets for supplying relief packages. When the drone visits any target location, it delivers one payload package. The energy equation (13) is a function of payload packages so, the energy required for the next visit will vary according to the changed payload weight as given in (13). The simulation is run 1000 times for each value of the grid size value. In each iteration of the simulation, the targets change their location. The grid size will be valid only if the charging stations corresponding to the specific grid size are accessible to the drones for recharging when they run out of power. The average minimum distance covered by the drones is calculated for each grid size value. The value of the cost function is calculated for different values of the grid size. The minimum value of the cost function determines the optimal value of the grid size. The number of charging stations determined by the optimal grid size is the optimal charging station. Table 1 shows the average minimum distance, charging stations, and cost function value against different values of the grid size.

In the first scenario, the number of targets is $M=39$. The disaster area is a square with sides of 40km each. The optimal charging stations are 25, corresponding to the optimal grid size value of 9.25km as shown in Table 1.

Table 1. Total distance and calculated cost function showing minima at 9.25km grid size

Scenario	Grid Size (km)	Charging Stations	Disatnce (km)	Cost Function
1	11	16	358.2359	518.2359
2	10	25	355.4964	605.4964
3	9.75	25	352.3604	602.3604
4	9.5	25	351.5633	601.5633
5	9.25	25	347.9187	597.9187
6	9	25	350.7462	600.7462
7	8	36	350.0603	710.0603
8	7	36	335.5975	695.5975
9	6	49	333.1546	823.1546

Figure 14 shows the graph of the grid size values versus the cost function. At a grid size value of 9.25km, we get the minima.

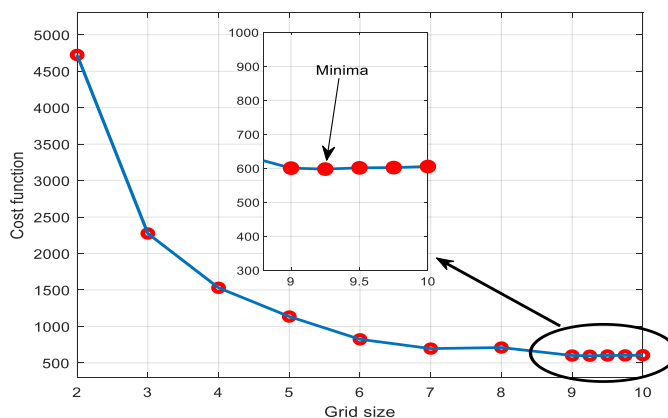


Figure 14. Simulation result showing minima at 9.25km in Grid size versus the cost function graph

In the second and third scenarios, simulations were done for the pre-disaster phase to get the optimal grid size value and the optimal charging stations for various sizes of the disaster area and the number of targets. In the fourth scenario, simulations were done for the post-disaster phase. The optimal routes were determined for the drones to supply relief items. The charging stations in this case are optimal charging stations determined in the pre-disaster phase.

In the second scenario, the number of targets is fixed to be $M=39$ and the size of the area is varied. Figure 15 shows the graph of the grid size values and the cost function values for different values of the size of the disaster area. The simulation is done with four different values of the area, i.e. square areas of sides equal to 45km, 40km, 35km, and 30km. The optimal grid size value in all the plots is the same as 9.25km as shown in Figure 14. The simulations show that the optimal value of the grid size is unchanged with the change in the size of the area.

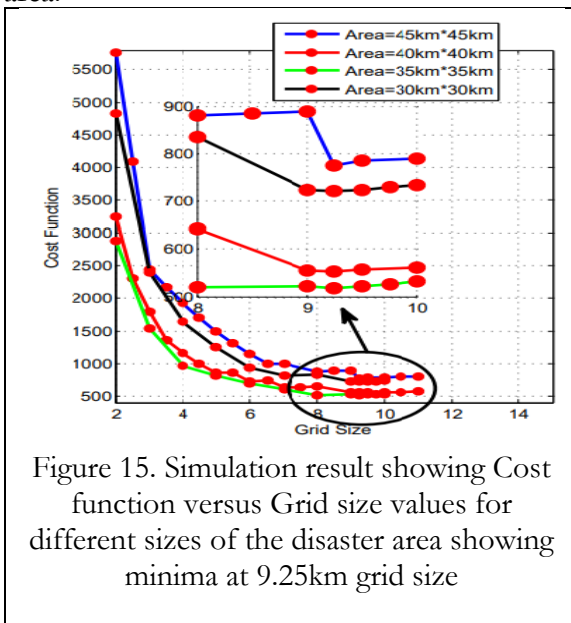


Figure 15. Simulation result showing Cost function versus Grid size values for different sizes of the disaster area showing minima at 9.25km grid size

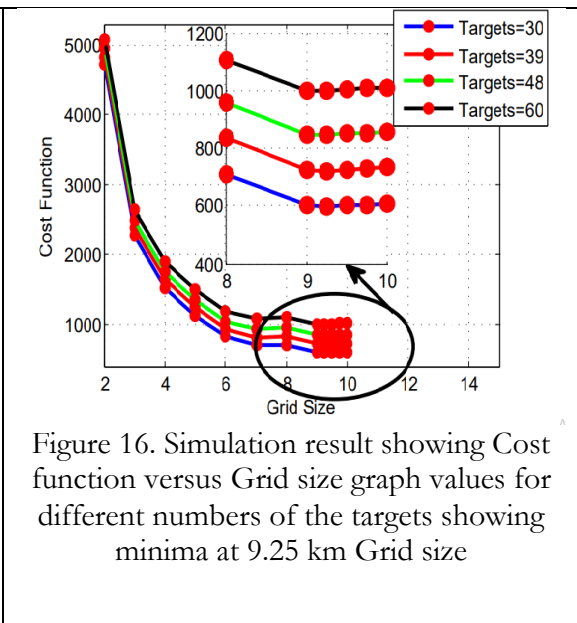


Figure 16. Simulation result showing Cost function versus Grid size graph values for different numbers of the targets showing minima at 9.25 km Grid size

In the third scenario, the area of the disaster is fixed, and the number of targets is varied. Fig. 16 shows the graph of the grid size values and the cost function values for the different numbers of the targets. The simulation is done with four different numbers of targets, i.e. 30, 39, 48, and 60. The simulation results indicate that the optimal grid size value in all the plots is the same as 9.25km as shown in Figure 15. The optimal value of the grid size is the same for different numbers of targets.

In the fourth scenario, the optimal routes of the drones are obtained. In this case, the number of the targets is kept equal to 39, and the size of the disaster area is kept equal to a square with sides 40km. The drone requires greater energy when it leaves the base station carrying the maximum payload, while it requires minimum energy when going back from the fifth target to the base station as it returns empty to the base station. The drone covers a larger distance when it is carrying lesser payload packages and vice versa. The number of optimal charging stations is 25. Figure 17(a), (b), and (c) show the optimal routes for the targets in the groups for three clusters.

The following parameters are needed for site selection as charging stations. R is the drone's maximum distance capacity with a full load and full energy. G is the grid size. We have optimized the value of the grid size, which determines the spacing between the adjacent charging stations. The location of the first charging station is at the origin where the x-coordinate is equal to zero and the y-coordinate is equal to zero and is taken as the reference location. The distance between the adjacent charging stations located along the x-axis direction is equal to the optimal grid size. Similarly, the distance between the adjacent charging stations located along the y-axis direction is equal to the optimal grid size. This formation leads to a grid of charging stations where the distance between the adjacent charging stations is equal to the optimal grid size.

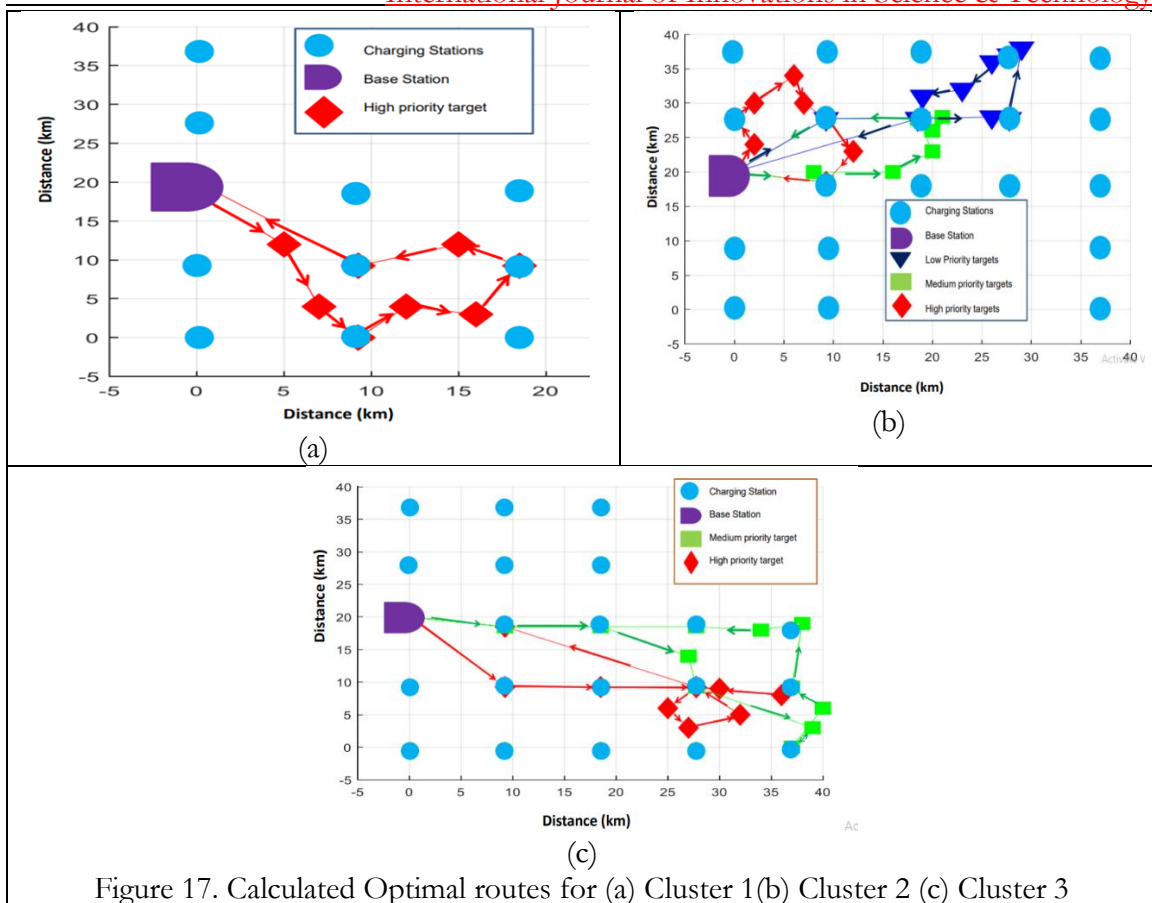


Figure 17. Calculated Optimal routes for (a) Cluster 1(b) Cluster 2 (c) Cluster 3

Discussions

Unmanned aerial vehicles (drones) come up with various applications. A bottleneck of drones is the limited flying time. Most commercial drones can only fly for about half an hour. According to the type of drones and the battery used, the max service distance without battery recharging ranges from 3 km to 33 km. For this reason, drone batteries should be periodically recharged in order to support long-distance drone flying. The limited flight time of UAVs, however, remains as a major challenge. Little is known about optimal methodologies to deploy charging stations. In literature, we find some studies that have addressed the problem of the deployment of charging stations. The authors have used different approaches to address this issue in the previous studies. In the next section, we will discuss the approaches used by authors in the existing literature and compare them with the proposed approach to validate our results.

In [26], the problem of deploying a number of charging stations to cover the customers in a demand area is investigated. Charging stations at optimal locations are deployed to get maximum customer coverage. For a customer located at a place that is unreachable by flying with a single battery, a drone can replace the battery at some charging stations and then fly again. For this reason, any two neighbor charging stations should be within a certain range such that a drone with a fully charged battery can reach one from the other. More generally, this requires that the deployed charging stations should be connected to the depot. Then, a drone that departs from the depot can arrive at any charging station via a subset of other charging stations, and it can further service the customer near this charging station. When the delivery task is completed, the drone can also return to the depot. this article focuses on the

problem of deploying a number of charging stations such that a certain percentage of customers in the demand area can be served by drones. A computationally efficient approach is proposed, which consists of an initial phase and an adjustment phase. In the first phase, a set of charging stations is deployed in a triangle pattern to fully cover the demand area; and in the second phase, the charging stations covering no or the least demand are removed, and the rest of the charging stations are repositioned. The adjustment phase repeats until no more charging stations can be removed. The main contribution of this work is the development of a charging station deployment method, which enables the drone delivery service to a certain number of customers.

In [27], the authors address the problem of deploying charging stations that maximizes the system performance, specifically concentrating on generating optimal UAV trajectories while minimizing the number of deployed charging stations. In this study, the authors formulated the problem of jointly optimizing UAV Trajectories and Locations of Battery swap Stations as an optimization problem and developed an optimization framework to solve the problem. Especially since finding the shortest trajectory for a single UAV visiting each region of interest and returning to the base station without even considering charging stations is essentially the traveling salesperson problem (TSP) which is NP-Hard, a heuristic solution called UBAT based on Ant Colony Optimization (ACO) is proposed to solve the problem. In [28], the authors consider the approach of deploying charging stations and collaborating with public transportation vehicles. The optimal deployment problem is formulated to minimize the average delivery time for the customers, which is a reflection of customer satisfaction. From the warehouse, which is far from a customer, a drone takes some public transportation vehicles to reach some position close to the remote area. When the customer is unreachable from the position where the drone leaves the public transportation vehicle, the drone swaps the battery at a charging station. In this study, in particular, it is assumed that there are some public transportation vehicles that pass the warehouse and the area of interest. Then, a drone can take these vehicles to reach the area. For a large area that cannot be covered by a drone without swapping its battery, deploying some charging stations in the area is taken into consideration. With the assistance of public transportation vehicles and charging stations, this strategy enables a drone to serve a remote customer. A new model is proposed in this study to characterize the flight distance for drones to serve customers, which is called the service model. Different from the commonly used coverage model, which says a customer is covered by a charging station within a certain range, the service model specifies the charging station via which a drone directly serves a customer in the shortest time. With this model, we formulate the charging station deployment problem from a simple case with only one charging station to a complex case with multiple charging stations.

In our proposed model, a simulation model was used to optimize the number and location of drone charging stations for deployment in a disaster-prone area in the pre-disaster scenario, aiming at the distribution of relief items to disaster-hit areas in the post-disaster scenario. To our best knowledge, we are the first to address the charging station deployment problem in a disaster-prone area. There is a need to install charging stations in the disaster-prone area in the pre-disaster phase, as access may be denied when the area is hit by disaster. Equation (1) gives the cost function, which depends upon the number of charging stations and the total distance. The flow chart given in Fig. 3 is used to find the minimum value of the

cost function. The minimum value of the cost function determines the optimal value of the grid size, which correlates to the optimal number of charging stations.

Limitations of the proposed model

In our model, we have assumed that the group size is five targets. If the number of targets is not a multiple of five, then some targets will be left ungrouped. As of now, we have considered only the flying mode of the drone in the energy equation. The proposed model does not take into account real-life constraints like the wind speed and other flight-related parameters of the drone. We have not considered the possibility that the charging station can be already occupied by a drone for recharging when another drone visits that charging station. We have allowed only one visit to a target location. If we consider multiple visits to a target location, the time at which the package is delivered will become a relevant parameter in the model.

Future work and recommendations

In future work, we can consider some parameters like the speed of the wind and other flight-related parameters of a drone to get more realistic simulations. The vertical take-off landing mode of the drone may also be considered in the energy equation. Multiple visits to a target location may be allowed to cater to a great demand of the target locations.

Conclusion

In this work, a simulation model was used to optimize the number and location of drone charging stations for deployment in a disaster-prone area. The relative priority of locations was considered, and preference was given to targets with higher priority levels. For the post-disaster phase, our model finds the optimal routes for the drones using data on the locations and the priority levels of the targets. We presented four scenarios to illustrate the use of our proposed model. Our simulations show that the optimal value of G (grid size) obtained in both scenarios was the same (9.25 km). It can be concluded that the optimal G is independent of the disaster-hit area, and it only depends on the drone's maximum distance capacity S . The presented research work can be applied in situations where relief supplies are needed to be provided swiftly to multiple locations hit by various kinds of disaster, including floods, earthquakes, avalanches, landslides, storms, etc.

References

- [1] A. Jabbarzadeh, B. Fahimnia, and F. Sabouhi, "Resilient and sustainable supply chain design: sustainability analysis under disruption risks," *Int. J. Prod. Res.*, vol. 56, no. 17, pp. 5945–5968, Sep. 2018, doi: 10.1080/00207543.2018.1461950.
- [2] "KIT - KIT - Media - Press Releases - Archive Press Releases - Natural Disasters since 1900: Over 8 Million Deaths and 7 Trillion US Dollars damage."
- [3] Y. Fukubayashi and M. Kimura, "Improvement of rural access roads in developing countries with initiative for self-reliance of communities," *Soils Found.*, vol. 54, no. 1, pp. 23–35, Feb. 2014, doi: 10.1016/J.SANDEF.2013.12.003.
- [4] J. Escribano Macias, N. Goldbeck, P. Y. Hsu, P. Angeloudis, and W. Ochieng, "Endogenous stochastic optimisation for relief distribution assisted with unmanned aerial vehicles," *OR Spectr.*, vol. 42, no. 4, pp. 1089–1125, Dec. 2020, doi: 10.1007/S00291-020-00602-Z/TABLES/7.
- [5] M. F. N. Maghfiroh and S. Hanaoka, "Multimodal relief distribution model for disaster response operations," *Prog. Disaster Sci.*, vol. 6, no. April, p. 100095, 2020, doi: 10.1016/j.pdisas.2020.100095.
- [6] S. Chowdhury, A. Emelogu, M. Marufuzzaman, S. G. Nurre, and L. Bian, "Drones for disaster response and relief operations: A continuous approximation model," *Int. J. Prod. Econ.*, vol. 188, pp. 167–184, Jun. 2017, doi: 10.1016/J.IJPE.2017.03.024.
- [7] X. Wei, H. Qiu, D. Wang, J. Duan, Y. Wang, and T. C. E. Cheng, "An integrated

- location-routing problem with post-disaster relief distribution," *Comput. Ind. Eng.*, vol. 147, p. 106632, Sep. 2020, doi: 10.1016/J.CIE.2020.106632.
- [8] M. Moshref-Javadi and S. Lee, "The customer-centric, multi-commodity vehicle routing problem with split delivery," *Expert Syst. Appl.*, vol. 56, pp. 335–348, Sep. 2016, doi: 10.1016/J.ESWA.2016.03.030.
- [9] S. M. R. Davoodi and A. Goli, "An integrated disaster relief model based on covering tour using hybrid Benders decomposition and variable neighborhood search: Application in the Iranian context," *Comput. Ind. Eng.*, vol. 130, pp. 370–380, Apr. 2019, doi: 10.1016/J.CIE.2019.02.040.
- [10] M. A. Ertem, M. İşbilir, and A. Şahin Arslan, "Review of intermodal freight transportation in humanitarian logistics," *Eur. Transp. Res. Rev.*, vol. 9, no. 1, pp. 1–11, Mar. 2017, doi: 10.1007/S12544-017-0226-Z/FIGURES/5.
- [11] A. Sebatli, F. Cavdur, and M. Kose-Kucuk, "Determination of relief supplies demands and allocation of temporary disaster response facilities," *Transp. Res. Procedia*, vol. 22, pp. 245–254, 2017, doi: 10.1016/j.trpro.2017.03.031.
- [12] T. I. Faiz, C. Vogiatzis, and M. Noor-E-Alam, "Robust Two Echelon Vehicle and Drone Routing for Post Disaster Humanitarian Operations," *arXiv*, no. January, pp. 1–44, 2020.
- [13] D. Rivera-Royero, G. Galindo, and R. Yie-Pinedo, "Planning the delivery of relief supplies upon the occurrence of a natural disaster while considering the assembly process of the relief kits," *Socioecon. Plann. Sci.*, vol. 69, p. 100682, Mar. 2020, doi: 10.1016/J.SEPS.2019.01.004.
- [14] C. C. Lu, K. C. Ying, and H. J. Chen, "Real-time relief distribution in the aftermath of disasters – A rolling horizon approach," *Transp. Res. Part E Logist. Transp. Rev.*, vol. 93, pp. 1–20, Sep. 2016, doi: 10.1016/J.TRE.2016.05.002.
- [15] S. Hu, C. Han, Z. S. Dong, and L. Meng, "A multi-stage stochastic programming model for relief distribution considering the state of road network," *Transp. Res. Part B Methodol.*, vol. 123, pp. 64–87, May 2019, doi: 10.1016/J.TRB.2019.03.014.
- [16] F. Sabouhi, A. Bozorgi-Amiri, and P. Vaez, "Stochastic optimization for transportation planning in disaster relief under disruption and uncertainty," *Kybernetes*, vol. 50, no. 9, pp. 2632–2650, 2020, doi: 10.1108/K-10-2020-0632/FULL/XML.
- [17] S. Baskaya, M. A. Ertem, and S. Duran, "Pre-positioning of relief items in humanitarian logistics considering lateral transshipment opportunities," *Socioecon. Plann. Sci.*, vol. 57, pp. 50–60, Mar. 2017, doi: 10.1016/J.SEPS.2016.09.001.
- [18] A. Moreno, D. Alem, and D. Ferreira, "Heuristic approaches for the multiperiod location-transportation problem with reuse of vehicles in emergency logistics," *Comput. Oper. Res.*, vol. 69, pp. 79–96, May 2016, doi: 10.1016/J.COR.2015.12.002.
- [19] J. M. Ferrer, F. J. Martín-Campo, M. T. Ortuño, A. J. Pedraza-Martínez, G. Tirado, and B. Vitoriano, "Multi-criteria optimization for last mile distribution of disaster relief aid: Test cases and applications," *Eur. J. Oper. Res.*, vol. 269, no. 2, pp. 501–515, Sep. 2018, doi: 10.1016/J.EJOR.2018.02.043.
- [20] P. H. V. Penna, A. C. Santos, and C. Prins, "Vehicle routing problems for last mile distribution after major disaster," <https://doi.org/10.1080/01605682.2017.1390534>, vol. 69, no. 8, pp. 1254–1268, Aug. 2017, doi: 10.1080/01605682.2017.1390534.
- [21] D. Kim, K. Lee, and I. Moon, "Stochastic facility location model for drones considering uncertain flight distance," *Ann. Oper. Res. 2018 2831*, vol. 283, no. 1, pp. 1283–1302, Dec. 2018, doi: 10.1007/S10479-018-3114-6.
- [22] H. Baharmand, T. Comes, and M. Luras, "Bi-objective multi-layer location–allocation model for the immediate aftermath of sudden-onset disasters," *Transp. Res.*

- Part E Logist. Transp. Rev.*, vol. 127, pp. 86–110, Jul. 2019, doi: 10.1016/J.TRE.2019.05.002.
- [23] C. Rottondi, F. Malandrino, A. Bianco, C. F. Chiasserini, and I. Stavrakakis, "Scheduling of emergency tasks for multiservice UAVs in post-disaster scenarios," *Comput. Networks*, vol. 184, p. 107644, Jan. 2021, doi: 10.1016/J.COMNET.2020.107644.
- [24] M. Won, "UBAT: On Jointly Optimizing UAV Trajectories and Placement of Battery Swap Stations," *Proc. - IEEE Int. Conf. Robot. Autom.*, pp. 427–433, May 2020, doi: 10.1109/ICRA40945.2020.9197227.
- [25] H. Huang and A. V. Savkin, "Deployment of Charging Stations for Drone Delivery Assisted by Public Transportation Vehicles," *IEEE Trans. Intell. Transp. Syst.*, 2021, doi: 10.1109/TITS.2021.3136218.
- [26] Y. Qin, M. A. Kishk, and M. S. Alouini, "On the Influence of Charging Stations Spatial Distribution on Aerial Wireless Networks," *IEEE Trans. Green Commun. Netw.*, vol. 5, no. 3, pp. 1395–1409, Apr. 2021, doi: 10.48550/arxiv.2104.01461.
- [27] S. Huma Ahmed Hassan, Syed Amer Mahmood, Saira Batool, Areeba Amer, Mareena Khurshid, Hina Yaqub, "Generation of Digital Surface Model (DSM) USING UAV/ QUADCOPTER," *Int. J. Innov. Sci. Technol.*, vol. 2, no. 3, pp. 89–107, 2020.
- [28] Y. Qin, M. A. Kishk, and M.-S. Alouini, "Drone Charging Stations Deployment in Rural Areas for Better Wireless Coverage: Challenges and Solutions," *IEEE Internet Things Mag.*, vol. 5, no. 1, pp. 148–153, May 2022, doi: 10.1109/IOTM.001.2100083.
- [29] X. Lin, Y. Yazcoglu, and D. Aksaray, "Robust Planning for Persistent Surveillance With Energy-Constrained UAVs and Mobile Charging Stations," *IEEE Robot. Autom. Lett.*, vol. 7, no. 2, pp. 4157–4164, Apr. 2022, doi: 10.1109/LRA.2022.3146938.
- [30] Y. Qin, M. A. Kishk, and M. S. Alouini, "Performance evaluation of uav-enabled cellular networks with battery-limited drones," *IEEE Commun. Lett.*, vol. 24, no. 12, pp. 2664–2668, Dec. 2020, doi: 10.1109/LCOMM.2020.3013286.
- [31] H. Huang and A. V. Savkin, "A Method of Optimized Deployment of Charging Stations for Drone Delivery," *IEEE Trans. Transp. Electrif.*, vol. 6, no. 2, pp. 510–518, Jun. 2020, doi: 10.1109/TTE.2020.2988149.
- [32] Jung, Sunghun and kim hyunsu, "Analysis of Amazon Prime Air UAV Delivery Service," *J. Knowl. Inf. Technol. Syst.*, vol. 12, no. 2, pp. 253–266, 2017, doi: 10.34163/jkits.2017.12.2.005.



Copyright © by authors and 50Sea. This work is licensed under Creative Commons Attribution 4.0 International License.